Available online at www.sciencedirect.com
SCIENCE DIRECT®
Journal of the European Ceramic Society 25 (2005) 997–1003
www.elsevier.com/locate/jeurceramsoc

Phase formation in porous liquid phase sintered silicon carbide: Part II: Interaction between Y_2O_3 and SiC

J. Ihle*, M. Herrmann, J. Adler

Fraunhofer-Institute for Ceramic Technologies and Sintered Materials, Winterbergstr. 28, 01277 Dresden, Germany

Received 10 December 2003; received in revised form 6 April 2004; accepted 22 April 2004
Available online 17 July 2004

Abstract

During the sintering of porous liquid phase sintered silicon carbide (porous LPS-SiC) a strong interaction with the atmosphere takes place, influencing the composition and stability of porous LPS-SiC components. The present paper is focused on the interaction of Y_2O_3 with SiC, which is part of the common used sintering additives for LPS-SiC (Y_2O_3–Al_2O_3–SiC). The interaction of Al_2O_3 and SiC has been studied in a previous paper [J. Eur. Ceram. Soc. (in press)].

The reaction products of the interaction of Y_2O_3 with SiC and the resulting microstructures were analysed using model experiments. The effects of the influence of different sintering atmospheres, namely Argon and Ar/CO, as well as vacuum and different temperatures have been investigated. The phase formation was determined by X-ray diffraction (XRD) and can be explained on the basis of thermodynamic calculations. Depending on the sintering conditions, silicides or yttrium carbides can be formed in addition to stable oxides, which can result in the decomposition of the samples after sintering. Reactions between SiC and Y_2O_3 during sintering can be suppressed successfully if an Ar/CO atmosphere is used.

Keywords: SiC; Liquid phase sintering; Phase development; Additives; Y_2O_3

1. Introduction

The solid state sintering of SiC (S-SiC) can be performed at very high temperatures up to 2200 °C with small additions of boron and carbon or boron, aluminium and carbon. In the case of LPS-SiC there is liquid phase formation due to Al_2O_3 and Y_2O_3 or other rare earth oxide additions, which subsequently accelerate the sintering in comparison to S-SiC. The sintering temperature can be decreased to 1800–2000 °C if the composition of the additives is close to the eutectic.[2,3]

The sintering conditions and the presence of a liquid phase during sintering have an essential influence on structure and phase composition, and subsequently the properties of the material. Beside the formation of yttrium–aluminium–garnet (YAG) as intergranular phase between the SiC grains, a reduction of the oxides by the silicon carbide can occur. Reactions between oxides and silicon carbide that result in the evolution of gases are associated with mass loss.

The properties of LPS-SiC have been observed and presented by several authors.[2–8] Groebner[9] has provided a thermodynamic assessment of the Gibbs energy functions for the phases in the system Y–Al–Si–C–O. A complete Gibbs energy data set was established for thermodynamic calculations in this quinary system.[9]

The decomposition of SiC during sintering by Al_2O_3 and Al_2O_3/Y_2O_3 mixtures was analysed by numerous authors.[1,2,5,6,10] The weight losses during sintering of SiC with Al_2O_3–Y_2O_3 additives result mostly from the evaporation of Al and Si suboxides. The sintering atmosphere influences the composition of the gas phase and consequently the extent of weight losses.[1,2,5,6] A common practice is the use of powder beds containing Al_2O_3 and SiC for minimising the mass loss by gas forming reactions during sintering of LPS-SiC.[3,4,6]

Baud et al.[6] described the evaporation of a SiC–Al_2O_3/Y_2O_3 mixture. They suggest a very similar behaviour in comparison to a pure SiC–Al_2O_3 mixture. In their thermodynamic calculations gaseous CO, SiO, Al_2O and Al are the main gas species. Additionally, there is a minor presence of gaseous Y and YO. Al_2O_3 and Y_2O_3 would react during

* Corresponding author. Tel.: +49 351 2553 682; fax: +49 351 2554 128.
E-mail address: Jan.Ihle@ikts.fraunhofer.de (J. Ihle).

0955-2219/$ – see front matter.
doi:10.1016/j.jeurceramsoc.2004.04.016

sintering to form either aluminates or a liquid oxide phase. In both cases the activity of Y_2O_3 would be less than one resulting in even smaller partial pressures of gaseous Y and YO.[6]

Cordrey et al.[4] investigated the sintering behaviour of silicon carbide with an yttrium oxide addition of 2 and 5 wt.%. During sintering the samples were surrounded in a coarse alumina and silicon carbide powder bed and contained within a carbon crucible. The authors observed that aluminium containing gas species react with the yttria to form a reactive liquid phase. The XRD analysis was inconclusive for identifying the resulting phases due to the small amount of additives. They concluded with the aid of energy dispersive spectroscopy (EDS) that Al, Y, Si and O are present in the secondary phase after sintering. The ratio of Al:Y:O in the secondary phase was determined by scanning Auger spectroscopy. In addition to the detected different ratios of Al:Y:O they assumed that an Al–Y–C–O compound and a Y–C–O compound may have formed.

The presence of yttrium silicates was detected by Hermanutz et al.[11] for hot-pressed SiC sintered with yttria. Y_2SiO_5, $Y_{4.67}(SiO_4)_3O$ and $Y_2Si_2O_7$ were formed in the bulk. Falk[7] observed a formation of $Y_2Si_2O_7$ as well as Si-O-rich glass pockets and graphite in capsulated hot isostatic pressed SiC samples with 1 wt.% Y_2O_3. The SiO_2 and carbon are likely constituents of the starting SiC powder and do not decompose due to the reduced decomposition rate under these conditions in comparison to normal sintering. Grande et al.[2] and Nagano et al.[12] concluded reaction (1)

$$SiC(s) + Y_2O_3(s) \rightarrow Y_2O(g) + SiO(g) + CO(g) \quad (1)$$

as a decomposition reaction of Y_2O_3 beside the main decomposition during sintering involving Al_2O_3. Because of a lack of data the thermodynamics of reaction (1) could not be appraised by Grande et al.[2] They did not measure a significantly reduced yttrium content in the secondary phase in LPS-SiC samples, and therefore have proposed that reaction (1) is not important for the weight loss.

Groebner[9] investigated the system Y–Si–C and has shown the silicides YSi_2 and Y_3Si_5 to be stable phases after synthesis at 1200 and 1500 °C. The carbon solubility of the silicides is low enough so that no alteration of the lattice constants was observed with an increase of carbon.[9]

In addition to the SiC lines, Grande et al.[2] found several weak diffraction lines in LPS-SiC samples maintained for 6 h at 1820 °C, which could not be attributed to a known phase. They proposed that a reduction of Y_2O_3 occurred after evaporation of Al_2O_3 resulting in carbide or oxy-carbide formation. By using EDS, the authors detected lower oxygen content in heat treated samples than that expected, by considering the amount of Y_2O_3 in the green samples. They considered the formation of oxy-carbides as the most probable reaction, due to the indicated release of gaseous SiO and CO after Al_2O_3 evaporation.[2]

Consequently, no conclusive information is available for the interaction of SiC and Y_2O_3 and therefore thermodynamical and experimental investigations are necessary for the understanding of the interactions during sintering.

The present paper is a study of the phase formation due to the dependence of the interaction of SiC and Y_2O_3 on temperature and gas atmosphere, and a comparison of the results with thermodynamic calculations.

2. Experimental

Samples with a higher content of oxides than the usual compositions of porous LPS-SiC were produced to enable a better detection of minor phases. A composition of 50 wt.% α-SiC (ESK F1200 green) and 50 wt.% Y_2O_3 (H.C. Starck grade C) was chosen. The samples were green pressed into tablets with a thickness of 5 mm and a diameter of 25 mm or bending bars with dimensions of 6 mm × 8 mm × 60 mm. All samples were sintered at 1 bar gas pressure or under vacuum (4×10^{-5} bar) in a graphite-heater furnace. The sintering conditions are shown in Table 1.

All samples were sintered in graphite crucibles. Graphite foil was placed between the crucibles and the samples in order to prevent adhesion of the samples to the crucible bottom by liquid formation during sintering. It was not possible to measure exactly the mass loss after sintering because some graphite foil was bonded to the samples after sintering. No mass loss results are therefore presented.

The phase composition of the samples was determined by X-ray diffraction analysis (XRD 7; Seifert-FPM; Cu Kα), using JCPDS standards.[13] Rietveld analysis (AutoQuan software) was used for the determination of the $Y_3Si_2C_2$ phase from XRD measurements. Optical microscopy and scanning electron microscopy with attached EDX (Leica Stereoscan 260) were used for an analysis of the microstructure of polished surfaces.

The FactSage® software package was used for thermodynamic calculations.[14] The necessary thermodynamic data for calculations were taken from the SGTE (Scientific Group

Table 1
Sintering temperatures, dwell time, atmospheres and resulting phase composition

Temperature (°C)	Dwell time (h)	Atmosphere	Phase composition of sintered samples
1850	1, 3, 5	Argon	Y_2O_3, α-SiC, $Y_3Si_2C_2$, YSi, (Y_xC_x)
1925	1	Vacuum	$Y_3Si_2C_2$, YC_2, α-SiC
1925	1	Argon + CO	Y_2O_3, α-SiC
1950	1	Argon	Y_2O_3, α-SiC, $Y_3Si_2C_2$, YSi, (YC_2)

Thermodata Europe) pure substance database (SGPS)[15] and solution database (SGSL)[16] as well as the special data set of the system Y–Al–Si–C–O from SGTE[17] based on the data set of Groebner.[9]

3. Results and discussion

3.1. Thermodynamic calculations

Table 2 shows the calculated equilibrium compositions of the Y_2O_3–SiC–Ar mixtures at 2223 K with different carbon contents or with additional CO, respectively. The calculations result in different compositions depending on the C, CO activity or the amount of argon used in the calculations. In all cases (excluding the high CO and low argon content) at least small amounts of condensed decomposition products of Y_2O_3 and SiC were found. The degree of decomposition increases with increasing volume of the gas phase. In the case of a high CO content in the atmosphere some additional carbon is formed.

In the experiments, the amount of carbon and the effective volume can not be properly predicted. Further detailed calculations were therefore carried out using compositions of 1 mol Y_2O_3, 5.6 mol Si, 5.4–6.1 mol carbon in steps of 0.1 and 1 mol argon. This correspond to a composition of 1.0 mol Y_2O_3 and 5.6 mol SiC with a range of a deficit of carbon up to −0.2 mol for the low carbon content and a additional carbon content of 0.5 mol for the high carbon content. The calculations were performed using a pressure of 0.1 MPa and a temperature range of 1950–2250 K. The results of the calculations are given in Figs. 1 and 2. The existence of a liquid metal C–Y–Si and/or a gamma phase consisting of Y–C–O was indicated under these conditions in a temperature range of 1950–2250 K (further calculations, which are not presented here, show similar results at 1850 K). Besides argon, the main gas species in the atmosphere in the temperature range of 1950–2250 K is CO. The partial pressure of SiO is very low in comparison to the CO partial pressure. The partial pressures of CO and SiO as a function of carbon content and temperature are plotted in Fig. 1a and b where it is shown that the partial pressure of CO increases with increasing temperature. The partial pressure of CO reaches 100 mbar at 2250 K without carbon additions and 176 mbar with a 0.5 mol carbon addition, i.e. only small changes takes place. The pressure of SiO is less than 10 mbar under these conditions, i.e. much lower than the CO pressure. If there is a deficit of carbon the SiO pressure is higher than for compositions with additional carbon and it increases up to 2100 K. At higher temperatures the SiO pressure decreases. The reason for this behaviour is the existence of Y_2SiO_5 up to 2100 K in equilibrium if there is a deficit of carbon. At higher temperatures no yttrium silicate was observed and therefore the partial pressure decreases (Figs. 1 and 2). The partial pressures of yttrium containing species are less than 10^{-6} bar at 2250 K. Therefore no drastic change of the yttrium content in the samples can be expected.

If there is an excess of carbon, a γ-phase consisting of yttrium, carbon and oxygen would be present already at lower temperatures in the calculated equilibrium composition, besides Y_2O_3 and SiC. Depending on the carbon content and the temperatures, the composition of the γ-phase changes between:

0.3383 mol Y		0.3440 mol Y
0.0006 mol O	and	0.0011 mol O
0.6611 mol C		0.6549 mol C

Under conditions where liquid metal, γ-phase, Y_2O_3 and SiC are present (low deviations of the SiC stoichiometry), the composition of the gas phase and the composition of the condensed phase do not depend on the carbon content (zero degrees of freedom).

Table 2
Results of thermodynamic calculations of equilibrium concentrations of the starting composition (5.6 mol SiC + 1.0 mol Y_2O_3) with different carbon or CO content and different amount of argon at 2223 K (1950 °C)

Phases	C = 0.001 mol			C = 1 mol			CO = 0.1 mol		
	Ar = 0.1 mol	Ar = 1 mol	Ar = 10 mol	Ar = 0.1 mol	Ar = 1 mol	Ar = 10 mol	Ar = 0.1 mol	Ar = 1 mol	Ar = 10 mol
SiC (mol)	5.589	5.489	4.486	5.599	5.592	5.126	5.598	5.595	4.632
Y_2O_3 (mol)	0.997	0.974	0.745	0.983	0.854	0.745	1.000	0.998	0.778
C (mol)	–	–	–	0.886	–	–	0.003	–	–
γ-Y–C–O (mol)	0.001	0.012	0.120	0.033	0.292	0.355	–	0.003	0.107
Liquid metal (mol)	0.015	0.161	1.619	–	–	0.645	–	–	1.395
C (mol fraction)	0.102	0.102	0.102	–	–	0.102	–	–	0.102
C (activity)	0.017	0.017	0.017	–	–	0.017	–	–	0.017
Si (mol fraction)	0.657	0.657	0.657	–	–	0.657	–	–	0.657
Si (activity)	0.265	0.265	0.265	–	–	0.265	–	–	0.265
Y (mol fraction)	0.241	0.241	0.241	–	–	0.241	–	–	0.241
Y (activity)	0.001	0.001	0.001	–	–	0.001	–	–	0.001
Ar (bar)	0.929	0.929	0.929	0.667	0.696	0.929	0.500	0.905	0.929
CO (bar)	0.066	0.066	0.066	0.327	0.299	0.066	0.491	0.090	0.066
SiO (bar)	0.005	0.005	0.005	0.006	0.006	0.005	0.009	0.005	0.005

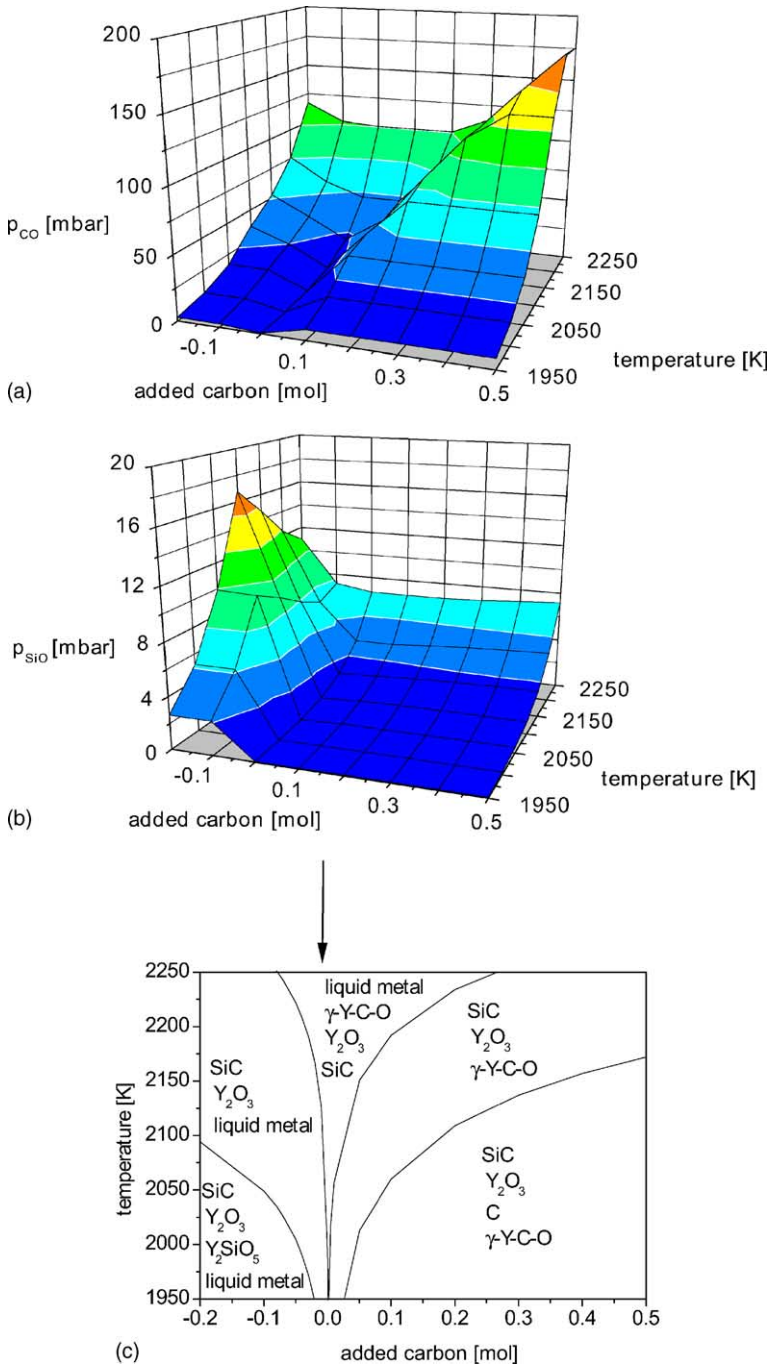

Fig. 1. Results of thermodynamic calculations of partial pressures as a function of carbon content and temperature in the calculated system Si–Y–C–O–Ar. Composition: 1.0 mol Ar, 1.0 mol Y_2O_3, 5.6 mol Si and 5.4, ..., 6.1 mol C. (a) Partial pressure of CO (b) partial pressure of SiO and (c) calculated condensed phases (the arrow indicates the stoichiometric composition of SiC and Y_2O_3).

The expected formation of a liquid metal and a gamma phase has to result in a different composition of Y_2O_3–SiC in samples of the model experiments after sintering. In the thermodynamic calculations the SiO_2 existing on the surface of the SiC-starting powder was not taken into account. From previous investigations it is known that it evaporates nearly completely at 1750–1950 K, e.g. below the temperature range considered in the calculations discussed here.

3.2. Experimental determination of the interaction

As shown in Table 1 different condensed phases were observed depending on the sintering conditions. Sintering in vacuum instead of in argon atmosphere was used for some experiments to accelerate the interaction. There was a rapid degradation of the vacuum sintered samples on exposure to air. In water, a heavy reaction accompanied by

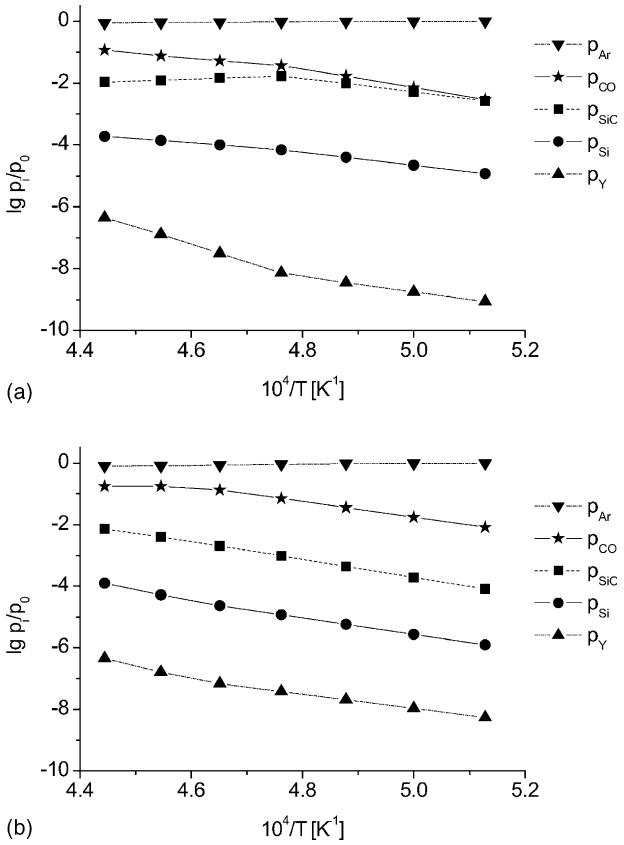

Fig. 2. Calculated partial pressures of gas species of the system Si–C–Y–O–Ar as a function of the inverse temperature ($p_0 = 0.1$ MPa). (a) Results of calculations with deficit of −0.2 mol carbon (condensed phases SiC, Y_2O_3, liquid metal for $10^4/T \leq 4.78$; above SiC, Y_2O_3, Y_2SiO_5, liquid metal). (b) Results of calculations with 0.5 mol added carbon (condensed phases SiC, Y_2O_3, γ-Y–C–O for $10^4/T \leq 4.60$; above SiC, Y_2O_3, C, γ-Y–C–O).

the evolution of gas was observed, resulting in a complete decomposition after only few seconds. In sealed samples YC_2 was determined as one of the major phases. After decomposition YC_2 disappears. The powder diffraction file of $Y_3Si_2C_2$ is not available in the JCPDF[13] and consequently a diffraction pattern for $Y_3Si_2C_2$ was generated from the structure data of Jeitschko et al.[18] for a XRD analysis of the unknown phase. Table 3 shows the *d*-values of the phase $Y_3Si_2C_2$ measured for a sintered sample after decomposition in water in comparison to the calculated *d*-values and intensities from the lattice constants and atomic parameters of $Y_3Si_2C_2$[18] Some of the lines show a superimposition with SiC and YSi diffraction peaks. Beside YC_2, $Y_3Si_2C_2$ is a main phase of samples sintered in vacuum (Fig. 3). In vacuum the Y_2O_3 was seen to be completely decomposed (Fig. 3).

All samples sintered in argon degraded completely in a few days, with exposure to air (Fig. 4), regardless of the sintering temperature. This indicates some decomposition of Y_2O_3 as predicted by the thermodynamic calculations and suggested by Grande et al.[2]

Table 3
Measured *d*-values of the phase $Y_3Si_2C_2$ in comparison to the *d*-values calculated from the lattice constants and atomic parameters by Jeitschko et.al.[18]

Measured values of $Y_3Si_2C_2$		Calculated values of $Y_3Si_2C_2$	
d-Value (Å)	Intensity	*d*-Value (Å)	Intensity
4.236	3	4.221	3
3.726	10	3.710	17
3.103	90	3.099	52
2.874	34	2.867	55
2.805	100	2.800	100
2.615	40	2.605	38
2.503	16	2.498	23
2.433	6	2.428	8
2.214	6	2.216	3
2.179	8	2.178	2
2.109	24	2.106	33
1.925	25	1.928	19
1.759	11	1.757	26
1.748	13	1.744	25
1.641	12	1.640	18

The samples sintered in argon consist of Y_2O_3, SiC (6H, 4H), $Y_3Si_2C_2$ and a small amount of YSi after decomposition in water. Yttrium carbide decomposed during exposure to water and therefore could not be detected (Fig. 5). The XRD analysis of samples not having been exposed to water before the measurement is very difficult. This is because of the expansion of the samples during the measurement caused by the reaction of the yttrium carbide with moisture in the air. The diffraction lines of YC_2 in the samples sintered at 1950 °C measured immediately after sintering are weak but could be detected clearly in sealed samples. Y_2C_3 as a second possible stoichiometry of yttrium carbide is assumed, because there are further weak diffraction lines matching the main lines of Y_2C_3. No diffraction lines of yttrium carbides were observed after exposure to water.

Kost et al.[19] describe the decomposition of yttrium carbides in water as being similar to that of calcium carbide. The structure of the YC_2 is the same as CaC_2 and, with the

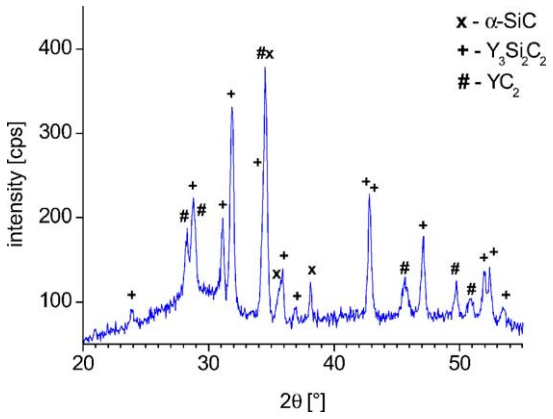

Fig. 3. Result of X-ray diffraction analysis of vacuum sintered sample at 1925 °C.

Fig. 4. Destructed samples of SiC–Y_2O_3.

reaction of water there is a formation of C_2H_2 and yttrium hydroxide. Other yttrium carbides like YC, Y_2C_3 and further compositions Y_xC_y show a similar behaviour and also decompose in water very quickly in a few minutes.[19,20] Mass spectroscopic measurements of porous LPS-SiC during the decomposition with atmospheric moisture indicate the presence of both H_2O (m18) and C_2H_2 (m26).[21] In accordance with Kost et al.[19] this is a reference to a decomposition of yttrium carbide.

The γ-YC_xO_y phase and the metal melt has a large area of homogeneity at high temperatures. During cooling different phases can crystallise from this solid solution. The oxicarbides and carbides which are stable at high temperatures decompose to yttrium carbide, yttrium silicon carbide, and in some cases yttrium silicides were formed. Therefore, the experimental findings agree at least qualitatively with the results of the thermodynamic calculations.

Additionally, a small contribution to the overall weight loss is caused by the formation of the SiO, which has a

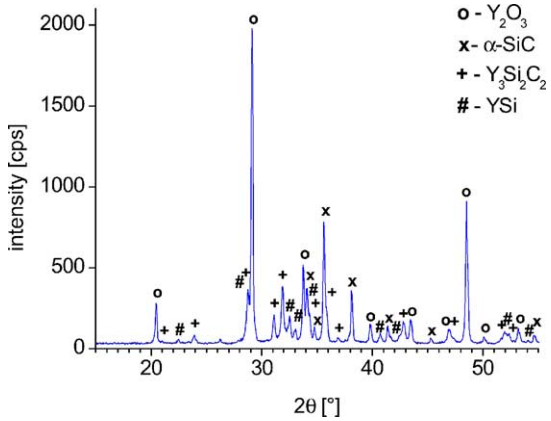

Fig. 5. Result of X-ray diffraction analysis of samples sintered in argon at 1850 °C for 5 h (after destruction in water).

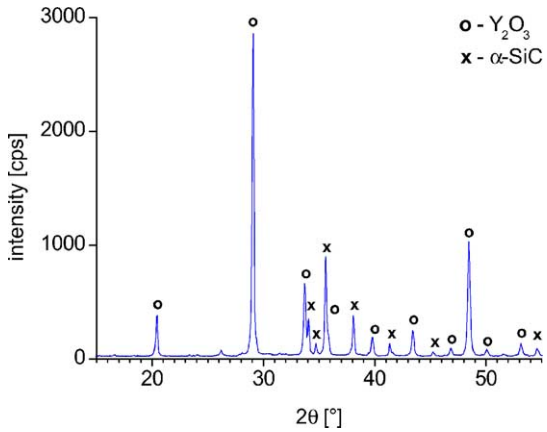

Fig. 6. Result of X-ray diffraction analysis of samples sintered in argon + CO at 1925 °C.

partial pressure of only 10% of that of CO. Y_2O has such a low partial pressure that a reduction of the amount of Y in the sample does not take place, but for sintering in graphite furnaces under an argon atmosphere a decomposition of the oxide to silicides and carbides takes place. It is possible to conclude from these findings that the decomposition of Y_2O_3 during sintering at 2223 K may be avoided with a CO partial pressure >100 mbar. This hypothesis was tested.

The results show that a stabilization of SiC and Y_2O_3 was achieved when a mixed atmosphere of argon with a CO partial pressure of 100 mbar was used. The samples sintered at 1925 °C in this mixed atmosphere at an overall pressure of 1 bar consist only of SiC and Y_2O_3 after sintering (Fig. 6).

4. Conclusions

Phase formation at temperatures in the range of 1850–2250 K was analysed with the aid of thermodynamic

calculations. The main gaseous species in the sintering atmosphere, beside Ar, was found to be CO. The partial pressure of CO increases with increasing temperature, and depends weakly on the carbon content of the samples within the limits investigated. The existence of a liquid metal C–Y–Si was indicated for a temperature range of 1950–2250 K up to an excess carbon content of approximately 0.25 mol. With increased carbon content, a formation of the γ-YC_xO_y phase was expected from the thermodynamic arguments.

Model experiments of the interaction of SiC with Y_2O_3 were performed, and these confirmed the thermodynamic findings qualitatively. These experiments have shown that, depending on the sintering temperatures and atmospheres, silicides or carbides (yttrium carbides) can be formed in addition to remnant silicon carbide and yttrium oxide. Two main decomposition products were $Y_3Si_2C_2$ in samples sintered in an argon atmosphere and YC_2 in vacuum sintered samples.

The sintering of SiC with Y_2O_3 in an argon atmosphere results in a complete degradation of samples after sintering during exposure to air. If the samples were sintered under vacuum this degradation occurs more rapidly. An explanation for this decomposition lies in the formation of yttrium carbides and oxy-carbides.

The reaction between SiC and Y_2O_3 during sintering can be suppressed successfully if a CO partial pressure is used, for which it has been shown that the post sintered samples only consist of the starting phases.

References

1. Ihle, J., Herrmann, M. and Adler, J., Phase formation in porous liquid phase sintered silicon carbide: I. Interaction between Al_2O_3 and SiC. *J. Eur. Ceram. Soc.* 2005, **25**, 987–995.
2. Grande, T., Sommerset, H., Hagen, E., Wiik, K. and Einarsrud, M.-A., Effect of weight loss on liquid-phase-sintered silicon carbide. *J. Am. Ceram. Soc.* 1997, **80**(4), 1047–1052.
3. Baud, S., Thévenot, F. and Chatillon, C., High temperature sintering of SiC with oxide additives: IV. Powder beds and the influence of vaporization on the behaviour of SiC compacts. *J. Eur. Ceram. Soc.* 2003, **23**, 29–36.
4. Cordrey, L., Niesz, D. E. and Shanefield, D. J., Sintering of silicon carbide with rare-earth oxide additions. *Sintering of Advanced Ceramics*, ed. C. A. Handwerker, J. E. Blendell and W. Kayser. The American Ceramic Society, Inc, Westerville, OH, 1990, pp. 618–636.
5. Schuesselbauer, E., Adler, J., Jaenicke-Roeßler, K. and Leitner, G., Sintering investigations on LPS-SiC. *Werkstoffwoche 98, Band VII*. 1999, pp. 207–212.
6. Baud, S., Thévenot, F., Pisch, A. and Chatillon, C., High temperature sintering of SiC with oxide additives: I. Analysis in the SiC–Al_2O_3 and SiC–Al_2O_3-Y_2O_3 systems. *J. Eur. Ceram. Soc.* 2003, **23**, 1–8.
7. Falk, L. K. L., Microstructural development during liquid phase sintering of silicon carbide ceramics. *J. Eur. Ceram. Soc*. 1997, **17**, 983–994.
8. Samanta, A. K., Dharguupta, K. K. and Ghatak, S., Decomposition reactions in the SiC–Al–Y–O system during gas pressure sintering. *Ceram. Int.* 2001, **27**, 123–133.
9. Groebner, J., *Constitution Calculations in the System Y–Al–Si–C–O*. Ph.D. thesis, University of Stuttgart, Germany, 1994.
10. van Dijen, F. K. and Mayer, E., Liquid phase sintering of silicon carbide. *J. Eur. Ceram. Soc*. 1996, **16**, 413–420.
11. Hermanutz, D. and Klemm, H., Effect of grain boundary composition on high temperature mechanical properties of hot-pressed silicon carbide sintered with yttria. *Ceramic Materials and Components for Engines*, ed. J. G. Heinrich and F. Aldinger. Wiley-VCH, 2001.
12. Nagano, T., Kaneko, K., Zhan, G.-D. and Mitomo, M., Effect of atmosphere on weight loss in sintered silicon carbide during heat treatment. *J. Am. Ceram. Soc.* 2000, **83**(11), 2781–2787.
13. Joint Committee on Powder Diffraction Standards, ASTM, Swartmore, 2001.
14. Bale, C. W., Chartrand, P., Degterov, S. A., Eriksson, G., Hack, K., Ben Mahfoud, R. *et al.*, FactSage thermochemical software and databases. *Calphad* 2002, **26**(2), 189–228.
15. *SGPS—SGTE Pure Substances Database*. Scientific Group Thermodata, Europe, 2000.
16. *SGSL—SGTE Alloy Solutions Database*. Scientific Group Thermodata, Europe, 1998.
17. *9288A00S—SGTE Si-Y-Al-C-O Database*. Scientific Group Thermodata, Europe, 2000.
18. Jeitschko, W., Gerde, M. H., Witte, A. M. and Rodewald, U. Ch., Subcell structure and two different superstructures of the rare earth metal silicide $Y_3Si_2C_2$, $Pr_3Si_2C_2$, $Tb_3Si_2C_2$ and $Dy_3Si_2C_2$. *J. Solid State Chem.* 2001, **156**, 1–9.
19. Kost, M. E., Schilow, A. L., Michewa, W. I. *et al.*, *Chemistry of Rare Earth Compounds*. Nauka, Moscow, 1983, pp. 69–95.
20. *Gmelin Handbook of Inorganic and Organometallic Chemistry (8th ed.), Rare Earth Elements, C 12a, Compounds with Carbon*. Springer-Verlag, 1995.
21. Ihle, J., *Structure and Properties of Porous Liquid Phase Sintered Silicon Carbide Ceramics*. Diploma thesis, Fraunhofer Institute for Ceramic Technologies and Sintered Materials, Freiberg University of Mining and Technology, 2000.